JACS
JOURNAL OF THE AMERICAN CHEMICAL SOCIETY

Article

pubs.acs.org/JACS

Organic Nanostructures on Hydrogen-Terminated Silicon Report on Electric Field Modulation of Dangling Bond Charge State

Peter M. Ryan,[†,‡] Lucian Livadaru,[†,‡] Gino A. DiLabio,*[,†,‡] and Robert A. Wolkow*[,†,‡]

[†]Department of Physics, University of Alberta, Edmonton, Alberta, Canada T6G 2E1

[‡]National Institute for Nanotechnology, 11421 Saskatchewan Drive, Edmonton, Alberta, Canada T6G 2M9

Supporting Information

ABSTRACT: We pursue dynamic charge and occupancy modulation of silicon dangling bond sites on H−Si(100)-2 × 1 with a biased scanning tunneling microscope tip and demonstrate that the reactivity and mechanism of product formation of cyclobutylmethylketone (CBMK) on the surface at the active sites may be thus spatially regulated. Reactivity is observed to be dependent on the polarity between tip and surface while the area over which reactivity modulation is established scales according to the dopant concentration in the sample. We account for these observations with examination of the competition kinetics applicable to the CBMK/H−Si reaction and determine how said kinetics are affected by the charge state of DB sites associated with reaction initiation and propagation. Our experiments demonstrate a new paradigm in lithographic control of a self-assembly process on H−Si and reveal a variant to the well-known radical mediated chain reaction chemistry applicable to the H−Si surface where self-assembly is initiated with dative bond formation between the molecule and a DB site.

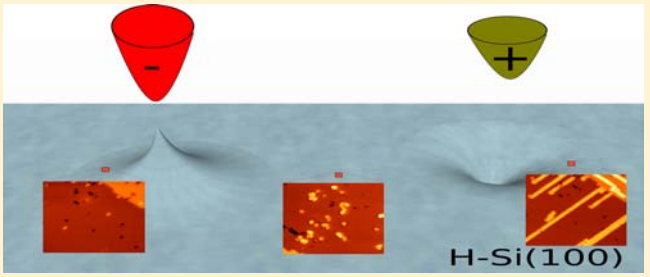

INTRODUCTION

Appreciation of the rich chemical, electrical and optical properties of surface defects, in particular dangling bond sites (DBs, unsatisfied valences on surface Si atoms) on semiconductor surfaces has risen tremendously over the past number of years and represents significant progress en route to the bottom-up fabrication of novel hybrid architectures. From the perspective of both fundamental and device applications, areas of study have included the fabrication, patterning, electronic properties, and chemical reactions of isolated DBs, DB wires, and clusters.[1−10] Motivated by the recently demonstrated ability of charged DBs on hydrogen terminated Si(100)-2 × 1 (henceforth H−Si) surfaces to selectively dictate reaction chemistry[11,12] and to exhibit inter-DB tunnel coupled relationships with potential for application in quantum cellular automata (QCA),[13] our studies have endeavored toward an understanding of how the charge occupation of surface DBs on H−Si surfaces may be modulated by external means.[14] We anticipate that dynamic influence over DB occupation could ultimately enable control of a wide range of processes from current gating[15] and information processing[16] in nanoscale structures to application in chemical catalysis.

Free from external influence, DB occupation on semiconductor surfaces is ultimately dictated by influences from bulk and interface electronic properties of the solid. Understood as localized states within the band gap of the semiconductor, DBs on H−Si pin the Fermi level of the crystal in the near surface region by accumulation of electronic charge (positive or negative). A band diagram representing an n-type semiconductor with an availability of such DB states is given in

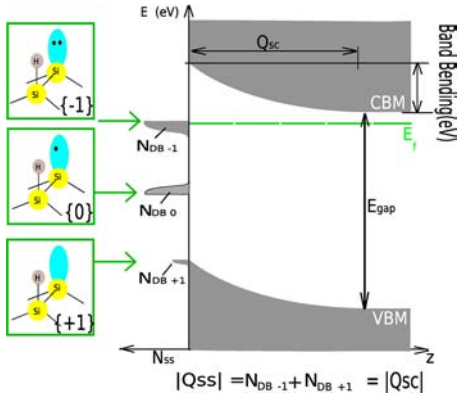

Figure 1. Band diagram schematic representing an n-type H−Si(100)-2 × 1 surface with an availability of DB sites represented by the blue lobes on the unterminated Si (100) surface atoms. Occupation number of the dangling bond state (−1, 0, +1) corresponds to the excess charge held at the site. Surface charge Q_{ss} resulting from positive and negative DB populations is compensated by the charge (Q_{sc}) established in a space charge layer of magnitude and extent determined by the Fermi level position with respect to the valence band maximum (VBM) and conduction band minimum (CBM) at the surface.

Figure 1. Under the condition that charge neutrality is upheld, the net charge density Q_{ss} of occupied and unoccupied DB sites is compensated by ionized bulk donors (Q_{sc}) in a subsurface

Received: February 21, 2012
Published: June 18, 2012

   dx.doi.org/10.1021/ja3017208 | J. Am. Chem. Soc. 2012, 134, 12054−12063

space charge layer. Moreover, the extent of charge transfer from the conduction band (CB), the width of the space charge layer and resulting charge state of DBs on the H−Si surface is set by the DB density and the location of the Fermi level at the surface.[17]

Low-temperature scanning tunneling spectroscopy (STS) enables the study of the local density of states (LDOS) associated with single DBs and clean Si dimers.[18] The LDOS varies with the particular charging state assumed by the DB (−1, 0, or +1), which in turn varies with the doping type and level in the sample. Depending on the temperature, observing the particular LDOS of the DB in the −1 or +1 states by STS may prove unfeasible, due to its decoupling from conductive channels.[18] Furthermore, the situation may become more complicated by a nonequilibrium charging effect of the DB if the charge transfer mechanisms in and out of the DB are of different physical nature and the associated rates are of different magnitude.[19]

To date modulation of DB occupation on H−Si has been implemented with static techniques whereby doping type and density, implanted in the semiconductor, shifts the Fermi level position with respect to DB states (e.g., highly doped n-type Si is known to facilitate high populations of negative DB sites[20]). Further to such procedures, Pitters et al.[14] have demonstrated localized DB occupancy modulation on H−Si by the fabrication of TiSi islands that act to perturb the surrounding electronic structure of the silicon through Schottky contact-established band bending. Neither of these approaches is amenable to dynamic control over DB occupation however. On the other hand, the electric field emanating from a tip utilized in scanning tunneling microscopy (STM) is known[13] to perturb the electronic structure in the semiconductor and therefore provides a convenient means for externally influencing DB occupancy with user specified control.

Many great ideas of STM manipulation of samples at the nanoscale were created in the early years of this new type of microscopy. Techniques that at present are quite widespread, such as field assisted manipulation of single atoms, electromigration, and sliding processes are outlined in now classical papers.[21,22] Manipulation of single atoms, molecules, and atomic clusters can be achieved both on metal and semiconductor surfaces. A combination of chemical and electrostatic interactions can be used to manipulate such entities.[23] The use of tip-induced electric fields is particularly appealing because it can be controlled by both the applied electric bias and the distance between the sample and the STM tip. Not only can atoms and molecules be removed and repositioned in this fashion, but chemical reactions such as single molecule synthesis can also be induced.[24] Isomerization reactions can be caused via tip-induced fields[25] or by inelastic tunneling currents.[26] Some more recent reviews on molecule manipulation and reaction control with the STM are found in refs 27 and 28.

In this manuscript, we pursue the biased STM tip approach to DB occupancy modulation on the H−Si surface and examine the spatial extent over which modulation is established for n-type H−Si samples of varying dopant density. To conduct our study it is desirable to develop a strategy that allows recording of the DB occupancy in areas on the surface subject to and absent from STM tip established perturbation of DB and bulk electronic states. A novel scheme employed in this manuscript is the use of DB occupancy-governed competition kinetics in the chain reaction chemistry known to occur for certain molecules at DB sites on the H−Si surface. Specifically, this is achieved here with the reaction of the molecule cyclobutylmethylketone (CBMK) on H−Si, which will be shown to act as an ideal probe of DB occupation by growth into self-assembled organic features with structure determined directly by tip established DB occupancy. STM imaging of local product concentration and resultant nanostructure shape serve to report on the occupation of DB sites subject to and absent from tip perturbation of electronic surface states for the duration of the molecular dose. Note that electronically and optically induced reactions on the H−Si surface can exhibit very complex dependencies on surface and subsurface processes;[29] therefore, a systematic study of these factors needs to be undertaken.

A prerequisite to understanding how CBMK may act as a reporter of DB occupancy on H−Si is an appreciation of the radical mediated chain reaction chemistry known to occur between sparse DBs on the H−Si surface.[30] Governed by two steps, the reaction is typically initiated by addition of a molecule through a C═C or C═O moiety to a surface DB, which results in the formation of a carbon centered radical intermediate that is bound to the surface. This is followed by a rate-limiting hydrogen atom abstraction from a nearby surface site, which passivates the radical intermediate and generates a new DB site that is available for a subsequent addition reaction. Both the silicon surface anisotropy and the structure of the addition intermediate participating in the radical-mediated growth determine the shape of the resulting nanostructure. For example, the carbon-centered radical formed upon addition of styrene to a DB on H−Si(100)-2 × 1 is *alpha* to the carbon atom that is covalently bonded to the surface. The short reach of the radical center and the 2 × 1 surface reconstruction limits the possible H abstraction sites to those neighboring the molecule addition site and this leads to the formation of linear nanostructures. Disordered organic nanostructures are produced in cases in which the addition intermediate contains a radical center that is more distant from the point of attachment to the surface than in the styrene example. The disorder arises because the long reach of the radical center allows for H abstraction from any one of a number of surface sites (not necessarily a site adjacent to the point of molecular attachment) and subsequent addition reactions do not place new surface-bound molecules next to existing ones. Isoprene (2-methyl-1,3-butadiene) is one example of a molecule that reacts with a surface DB to produce disordered nanostructures according to our previous STM observations.[31]

Given these considerations, it is clear that mechanistic information about radical-mediated reactions on H−Si can be obtained through STM observations of the types of nanostructures (linear or disordered) that are formed on the surface. One avenue for achieving this is to expose the surface DBs to a molecule that forms an intermediate upon addition to a surface DB that may rearrange prior to abstracting a hydrogen atom from the surface. In such a case, the resulting nanostructure shapes directly report on the pathway along which the addition intermediate reacted. In this work, we exploit the ability of the intermediate formed by the reaction of CBMK, see Figure 2 with a surface DB to undergo a ring-opening reaction prior to H abstraction. In analogy to styrene, CBMK forms a carbon-centered radical intermediate upon addition to a neutral DB on H−Si. The intermediate (II) then reacts by one of two possible pathways: The *alpha* radical (II) can either abstract a hydrogen atom with rate constant k_H(II) from a site on a neighboring dimer in the same row (indicated

dx.doi.org/10.1021/ja3017208 | J. Am. Chem. Soc. 2012, 134, 12054−12063

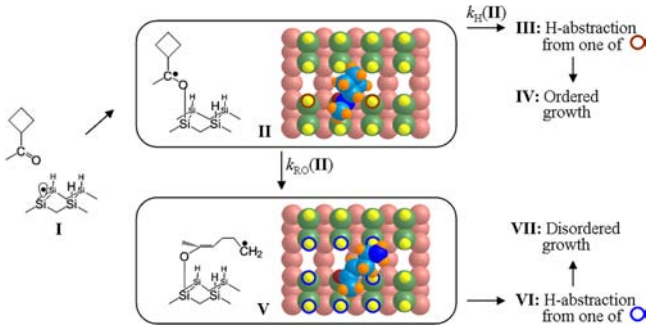

Figure 2. Competitive reaction pathways for cyclobutylmethylketone on models of hydrogen-terminated silicon(100)-2 × 1. The two reaction pathways available to the CBMK intermediate (II) are described fully in the text. Color key: Subsurface Si = salmon, surface Si = green, silicon surface H = yellow, O = red, nonradical carbon = light blue, carbon-centered radical = dark blue, molecule H = orange.

by brown circles in Figure 2), which leads to linear nanostructure formation. Alternatively, the intermediate can undergo a well-characterized ring-opening[32] with rate constant k_{RO}(II) to generate an *epsilon* radical (V) that is capable of abstracting an H atom from one of several surface sites (indicated by blue circles in Figure 2). The new surface DB sites so generated are randomly positioned relative to the point of CBMK attachment and so subsequent addition/ring-opening/abstraction reactions generate disordered structures.[33] Density-functional theory calculations (vide infra) reveal that the room-temperature hydrogen atom abstraction by the ring-closed intermediate has a rate constant that is nearly the same as the rate constant associated with the process of radical ring-opening. The nearly perfect balance between the two processes (immediate H abstraction vs ring-opening followed by H abstraction) suggests that CBMK would perform as a sensitive probe to factors, including DB occupancy, that influence radical-mediated chain reaction chemistry on H−Si.

EXPERIMENTAL AND COMPUTATIONAL METHODS

STM measurements were performed in an Omicron VT-STM/AFM with a base pressure of 9×10^{-11} Torr. Samples used included three routinely prepared[34] H-terminated Si n-type crystals of resistivity 0.003 Ω cm, 0.1 Ω cm, 1Ω·cm corresponding to sample arsenic concentrations of 10^{19} (high doped (HD)), 10^{17} (medium doped (MD)), and 10^{15} (low doped (LD)) atoms/cm^3. CBMK was purchased from Sigma-Aldrich (>99% purity) and introduced into the vacuum chamber through a variable leak valve following several freeze−

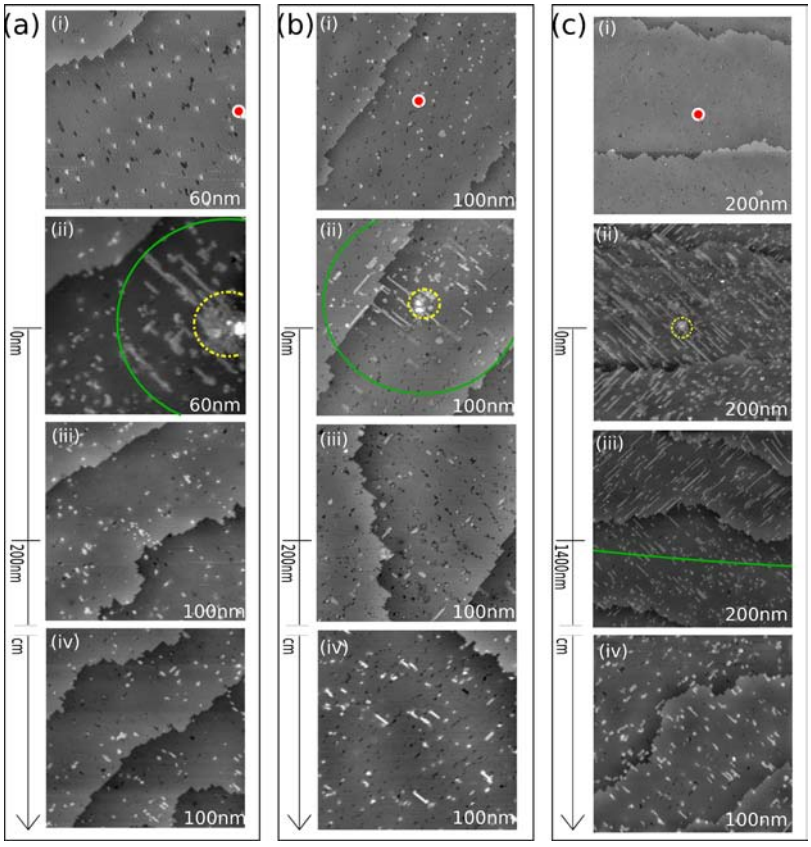

Figure 3. Series of STM images recorded on (a) high doped (HD), (b) medium doped (MD) and (c) low doped (LD) H−Si samples before and after reaction with the CBMK molecule. STM images (i) are recorded predose while STM images (ii), (iii) and (iv) are recorded post CBMK dose. For each of the data sets, the STM tip was maintained at 100 pA and −4 V with respect to the grounded sample for the duration of the dose at the location marked by the red dot in STM image (i). The scale positioned alongside STM images (ii), (iii) and (iv) indicates the distance from the reference location on the sample (red dot in i) where each STM image is recorded post CBMK dose. The yellow circle in STM images (ii) shows areas of product debris where CBMK has reacted on unterminated Si. The green boundary indicates the area on each sample inside of which well ordered nanostructure formation from the reaction of the CBMK on H−Si is observed. Outside the green boundary quasi ordered CBMK nanostructures are the primary products of the radical mediated chain reaction. In all cases, the radii established are to within a ca. order of magnitude. Distances shown in the bottom right corners of the images represent widths.

dx.doi.org/10.1021/ja3017208 | J. Am. Chem. Soc. 2012, 134, 12054−12063

pump−thaw degasification steps. Following caracterization of the pristine H−Si surfaces the STM probe was set stationary with defined tunneling conditions (I_t = 100 pA,V_{tip} = ± 4 V) while samples were exposed to a 100 L dose (1×10^{-6} Torr for 100 s) of the CBMK molecule. Chamber pressure was then allowed to recover over a period of several hours to 2×10^{-10} Torr before tunneling conditions of the STM tip were adjusted and scanning allowed to commence. STM images of the reacted surface were then obtained along a fixed coordinate with successive displacement increments from the location where the tip was held during the molecular dose (henceforth described as the reference location). Tunneling conditions set during characterization of the postdose surface, with typical parameters of V_{tip} = 2.2 V and I_t = 100 pA, were chosen so as to not disturb product structures. A single (macroscopic) STM tip was used for all of the measurements presented in this study, and H−Si samples were maintained at room temperature throughout experiments. We point out that all experiments were repeated several times with various dosing and tip conditions. Data was collected over large areas and numerous measurements were done to confirm our findings.

All calculations were performed using the Gaussian-03 suite of programs.[35] The contributions to the components of the Arrhenius rate constants were obtained from calculations performed in stages. The first stage involved a large model for H−Si(100)-2 × 1 surface comprised of 71 Si atoms and consisting of two dimer rows each containing four dimers and six layers (see Supporting Information, SI). The Si−Si backbonds that were cleaved to construct the model were terminated by H atoms, whose Cartesian coordinates were kept fixed throughout all of the calculations. Surface dangling bonds were terminated by H atoms, where appropriate. This cluster was used to model the structure and energetics associated with the reaction of a CBMK with the surface at a dangling bond site that was on the same side of a dimer row and on the next dimer relative to a site at which a CBMK had undergone an addition/abstraction reaction. This was done in order for the calculations to capture the possible influence of noncovalent interactions between surface-bound molecules on reaction energetics. The modeling was performed using the B971[36] density-functional theory method with the 6-31G(d) basis sets on Si atoms and 6-31+G(d,p) basis sets on all other atoms.[37] Dispersion-correcting potentials were applied to all C[38] and Si[39] atoms to more accurately model the effects of noncovalent interactions.

In the second stage of calculations, ring-opening and H-abstraction barriers obtained using the large model were augmented by energy corrections obtained for smaller models of the reaction centers (see SI) using the CBS-QB3 complete basis set approach of Petersson et al.[40] The models utilized were obtained by eliminating all atoms in positions beyond "beta" to the reaction site with the restriction that a contiguous model be used. The model for ring-opening had the chemical formula $C_6H_{13}OSi$ and for H-abstraction the chemical formula was $C_3H_{17}OSi_5$. The structures of the small models were kept frozen at the large model, B971-determined structures. Energy corrections to barrier heights were then determined by the difference between the CBS-QB3 energies and energies obtained from the same B971 computational treatment used for the large structures. These corrections, which were added to the barriers obtained from the first stage of the calculations, were computed to be 1.26 (ring-opening) and 0.77 (H-abstraction) kcal/mol.

The third stage of the calculations involved the determination of vibration corrections and partition coefficients. For these we used a four dimer cluster consisting of 27 Si atoms (see the SI). The Si backbonds in this model were capped with quantum capping potentials,[41] which are artificial Si atoms designed to reproduce Si−Si bonds. Structures were fully optimized using the same computational approach as was used in stage one for the large models. All minimum energy structures had positive vibration frequencies, whereas all transition state structures had a single imaginary frequency that connected reactants to products.

Kinetic information on the ring-opening and H-abstraction applicable to the bound CBMK intermediate were determined by using the data from the calculations described above with conventional transition state theory. The ring-opening rate constants were multiplied by a factor of 2, reflecting two equivalent C−C scission pathways. The effect of hydrogen atom quantum mechanical tunneling was determined using the Eckart approach.

■ EXPERIMENTAL RESULTS

Figure 3a, b and c shows sequences of pre (i) and post (ii−iv) CBMK dose STM images on the HD, MD and LD H−Si samples respectively. For each of the data sets presented in Figure 3, the STM tip was maintained at 100 pA and −4 V with respect to the grounded sample for the duration of the dose at the location marked by the red circle in image (i). For the HD sample in Figure 3a, comparison between STM images (i) and (ii) reveals that the presence of the biased tip during reaction facilitates ordered growth of CBMK lines up to 20 nm long over a region of radius $r \approx 30$ nm from the reference location. A green line defining the area of tip established perturbation circumscribes the ordered nanostructures and represents a boundary outside of which the majority of assembled nanostructures exhibit structural orientation non reconcilable with the templating influence traditionally imparted by the anisotropy of the Si(100) (2 × 1) surface. For Figure 3b and c, similar tip established perturbations to the CBMK reaction on H−Si are observed with respective areas of reactivity modulation increasing slightly to $r \approx 50$ nm for the medium doped crystal and to a substantial $r \approx 1400$ nm value on the low doped surface. We note that for each data set shown in 3, within the locality of tip influence there is in addition to the ordered CBMK lines running parallel to the Si dimer row directions, significant product debris that has reacted directly under the STM tip (yellow circle) without necessarily participating in radical mediated line growth process. It is likely that this material results from reaction of the CBMK molecule upon areas of nonhydrogen terminated Si with the STM tunneling conditions responsible for the localized hydrogen desorption via vibrational excitation of the Si−H bonds.[6,42]

Outside the green boundary determined for each of the data sets in Figure 3, we observe a relative inability of the CBMK molecule to participate in the radical mediated reaction on the H−Si surface compared to that of the molecule recorded in regions of tip influence. Broadly differentiable by a decrease in both nanostructure length and compositional organization wherein nanostructures are observed to meander across multiple Si dimer rows we classify the CBMK products fabricated under such conditions as quasi ordered. The limited and quasi-ordered growth of the CBMK molecule in these locations is illustrated with greater clarity in Figure 3a−c using high resolution STM images of the post CBMK dose H−Si surfaces recorded at surface coordinates centimeters away from the respective reference locations given in Figure 3. For the HD, MD, and LD H−Si surfaces in Figure 4a, b, and c, respectively, orange arrows indicate CBMK structures that have grown in a quasi-ordered fashion rather than traversing the Si dimer row directions aligned perpendicular to one another on alternate terraces. Accounting for such an assembly mode of the molecule in these regions of negligible tip perturbation to surface states involves scrutiny of possible mechanisms of H-atom abstraction available to the CBMK molecule en route to product formation and is undertaken below.

In Figure 5, we examine how the tip polarity set for the duration of the CBMK reaction, affects local nanostructure formation on the LD H−Si surface. Prior to collection of the data set shown in Figure 5a the STM tip is set stationary with

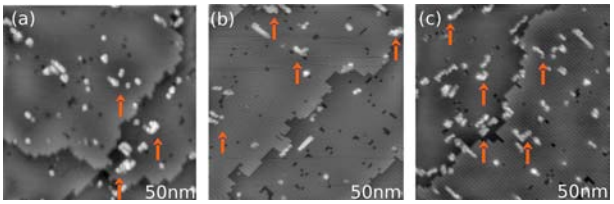

Figure 4. High resolution STM images of CBMK quasi ordered structures recorded on (a) HD, (b) MD and (c) LD H−Si samples post dose. Each image is obtained a few centimeters outside the point of reference indicated by the red dot in Figure 3. Orange arrows indicate CBMK structures that are seen to meander across multiple dimer rows. Distances shown in the bottom right corners of the images represent widths.

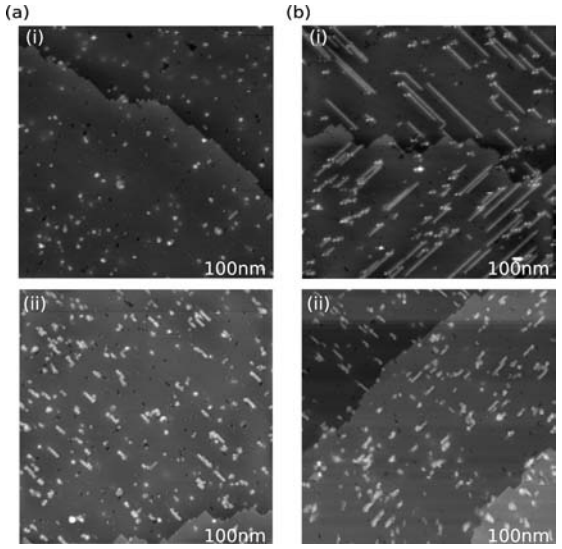

Figure 5. For (a) and (b), STM images (i) and (ii) are both recorded post a 100 L dose of the CBMK molecule on an LD H−Si sample. The reaction in (a) is carried out on a forward biased sample (tip at +4 V) whereas the reaction in (b) is carried out on a reverse biased sample (tip at −4 V). In (a), STM image (i) is recorded inside the area of tip perturbation where negligible growth of the molecule is observed due to the biasing conditions. In (b), STM image (i) allows observation of ordered CBMK lines following the CBMK reaction under a negative tip. Outside regions of tip perturbation, STM image (ii) in (a) and (b) both show quasi-ordered products of the CBMK on H−Si reaction determined characteristic in the absence of tip perturbation. Distances shown in the bottom right corners of the images represent widths.

tunneling conditions 100 pA and +4 V above the H−Si sample. Following the 100 L molecular dose, STM images (i) and (ii) were recorded at respective locations within ($r \approx 1400$ nm) and outside ($r \approx 1$ mm) the locality of tip influence identified for the low doped H−Si surface in Figure 3c. For comparison, Figure 5b provides STM images recorded at equivalent locations on a second sample post a CBMK dose where the tip was maintained at 100 pA and −4 V for the duration of the reaction. In STM image (i) for Figure 5a, we observe in the vicinity of tip influence, negligible participation of the CBMK molecule in the radical mediated reaction on the H−Si surface. We point out that tip shadow effects introduce some uncertainty in the dosing pressure. The negligible reactivity of the surface consistent with STM image (i) is observed across a region of $r \approx 1600$ nm from the reference location established prior to the CBMK dose. This result when compared to STM image (i) for Figure 5b indicates that the polarity of the STM tip effectively regulates the CBMK reaction on H−Si over a defined locality with a positive tip deactivating the reaction and a negative tip promoting ordered growth of the molecule. Outside the region of tip influence (STM images (ii) in Figure 5a and b) the CBMK products show quasi ordered growth as described earlier. Experiments with the positively biased tip were not pursued extensively in our study because it was found early on that they do not stimulate molecular line growth, or even distorted growth. Therefore, we chose to focus more extensively on experiments with negatively biased tip and studied the ensuing molecular structures.

As an additional note, tip structural changes during an STM experiment have been known to affect its desorption effectiveness.[43] During our experiments, if nanoscopic tip changes occurred they did not reflect in the outcome of observed CBMK reaction products.

COMPUTATIONAL RESULTS

The experimental results presented above show three outcomes to the CBMK on H−Si reaction dependent upon the condition of the DBs that the molecule encounters en route to product formation. In the absence of any tip perturbation to DB sites, quasi ordered growth of the molecule is observed to be the preferred consequence of the reaction. Under tip influence and orchestrated by conditions of forward bias (negative sample polarity), DBs appear to undergo negligible reaction. Conversely under conditions of reverse bias (positive sample polarity), facile and ordered assembly of the molecule on the surface is observed. To understand the behavior of the CBMK on H−Si reaction under such conditions we study with DFT the energetics and kinetics of the process illustrated in Figure 1. The ring-opening rate constant for the addition intermediate at $T = 300$ K k_{RO}^{300} was calculated to be 2.2×10^2 s^{-1}, a value that is consistent with the expectation that the measured solution-phase rate constant for the ring-opening of cyclobutyl methyl, 5×10^3 s^{-1},[44] will be reduced by about an order of magnitude because of the radical stabilization effects of a methyl and a siloxyl substituent at the radical center (c.f. k_{RO}(cyclopropyl methyl) = 1.3×10^8 s^{-1}, k_{RO}(α-trimethylsiloxycyclopropyl methyl) = 2.4×10^7 s^{-1}).[45,46] The calculated result for the rate of H atom abstraction for the ring closed intermediate k_H^{300} is only slightly higher than k_{RO}^{300} with a value of 2.68×10^2 s^{-1}. Collectively, these data predict that upon formation of the addition intermediate, and in the absence of any external perturbation, both the ring-opening and direct H abstraction mechanisms are accessible to the CBMK moiety en route to nanostructure formation. We propose here that the small differences in the kinetics for both mechanisms are responsible for the observation of quasi ordered CBMK assembly at sample locations subject to negligible tip influence for the duration of the reaction and recorded in the STM data of Figures 3−5.

Accounting for the negligible reaction of the CBMK molecule on H−Si under conditions of negative sample bias, we consider the likely charge state of the DB encountered by the incoming molecule. In recent work,[11] it was shown that the Fermi level determined populations of negatively charged DBs on H−Si exhibit low reactivity with styrene due to electrostatic repulsion between the DB center and the C=C π bond of the incoming molecule. We propose that under negative sample bias conditions the majority of DBs under tip influence will hold a net negative charge. The resulting electrostatic repulsion interaction between the negatively charged DB center and the lone-pairs of electrons on the oxygen atom of the CBMK

dx.doi.org/10.1021/ja3017208 | J. Am. Chem. Soc. 2012, 134, 12054−12063

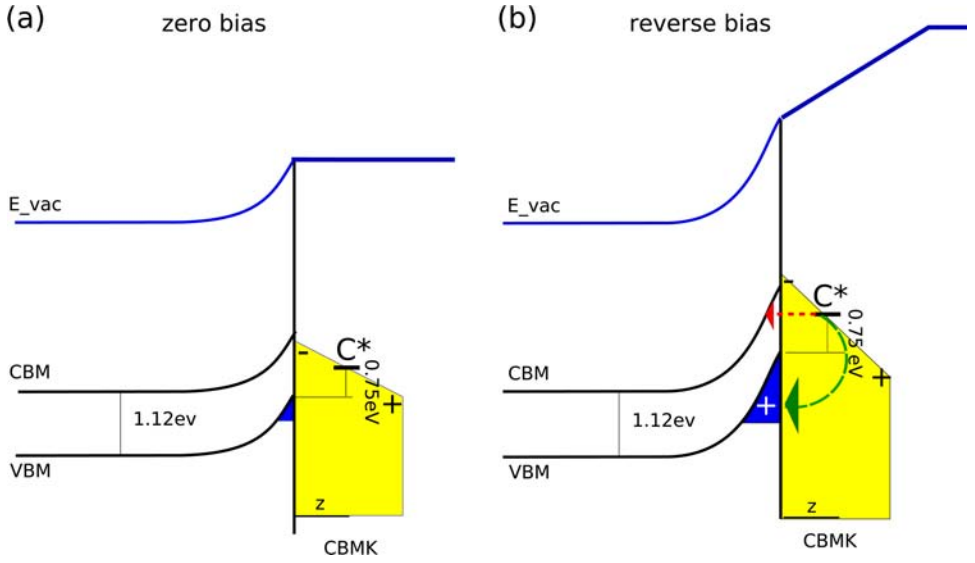

Figure 6. Energy band schematics appropriate for the CBMK intermediate tethered to an n-type H−Si surface under conditions of (a) zero bias and (b) positive sample bias respectively. The SOMO level (C*) of the CBMK intermediate is positioned above the CBM of the surface at a distance z ≈ 2 Å from the interface, and the upward band bending in the space charge layer is increased under the influence of a negative tip. Electron tunneling (red arrow) from the C* level to the CB of the surface is inhibited by an interplay of vacuum and molecular dipole barriers represented by a blue line and yellow trapezoid respectively. Recombination events (green arrow) more probable under condition of positive sample bias offer a second mechanism by which CBMK carbocation formation is facilitated.

molecule will raise the barrier to formation of the addition intermediate and curb the radical mediated growth process at the first step in the reaction.

In our endeavor to understand the behavior of the CBMK on H−Si reaction under conditions of positive sample bias, we examined the electronic structure of the surface bound CBMK intermediate. An important trait of the system, identified through wave function analysis concerns the energetic placement of the singly occupied molecular (SOMO) level in the intermediate structure. The SOMO state labeled as C* in Figure 6 and predicted by our DFT calculations to reside 0.75 eV[47] above the valence band maximum (VBM) of the H−Si surface establishes itself as a second variety of mid gap state in the electronic structure of the molecule-surface system. In anticipation that electron transfer from the C* state is a viable process with C* occupation determined by the same factors that govern DB occupation, we calculated the energetics associated with the ring-opening and hydrogen atom abstraction of a bound CBMK carbocation intermediate. Reoptimisation of the converged neutral intermediate structure under conditions of enforced positive charge alters the Si-CBMK binding from a covalent Si−O bond, wherein the associated carbonyl C is a radical center, to a dative bond between the empty (positive) DB state and the lone-pair of electrons on the oxygen atom of the CBMK molecule. The barrier for ring-opening of the datively bound species is predicted by DFT to be very high (>40 kcal/mol, as expected for the formation of a carbocation) and therefore the process is extremely unlikely. Conversely, hydrogen abstraction by the ring closed carbocation is competent with a predicted barrier of 18 kcal/mol. This is only 4 kcal/mol higher than the H abstraction barrier predicted for the neutral case and comparable to that calculated for the facile styrene line growth reaction on H−Si.[48]

SEMIEMPIRICAL MODEL FOR SURFACE CHARGE DISTRIBUTION

The DFT results outlined above predict that on formation of a CBMK carbocation intermediate, ring-opening and consequent quasi-ordered growth of the CBMK molecule on H−Si will be inhibited in favor of ordered assembly. Furthermore, experiment has shown that ordered growth of the CBMK molecule is observed only under a negative tip. Given this information it is warranted to question how CBMK carbocation formation might be promoted under positive sample bias conditions. In Figure 6a and b, we show energy band schematics appropriate for the CBMK intermediate tethered to an n-type H−Si surface under conditions of zero bias and positive sample bias, respectively. The C* level in each schematic is positioned 0.75 eV above the VBM of the surface at a distance of z (∼2 Å) from the interface and the upward band bending in the space charge layer is increased under the influence of a negative tip (Figure 6b). To account for charge transfer processes from the C* state to the semiconductor bulk with potential to establish a carbocation CBMK intermediate, respective red and green arrows depicting electron tunneling and electron hole recombination events are drawn in Figure 6. Noting that the electron tunelling to the CBM of the bulk is only thermodynamically inclined for tip established band bending in excess of 0.37 eV and is further subject to vacuum and dipole potential barriers[49,50] (represented in Figure 6 as a blue line and a yellow trapezoid respectively) that act in conjunction with a space charge barrier to collectively establish the decay length of the C* wave function we expect that a electron transfer by a tunelling mechanism is highly unlikely even under conditions of positive sample bias.

In contrast to electron tunelling and recognizing the correlation that under positive sample bias conditions, subsurface hole concentration will be enhanced (see Figure 6b) we anticipate that electron hole recombination events establish a primary route by which the CBMK molecule may

dx.doi.org/10.1021/ja3017208 | J. Am. Chem. Soc. 2012, 134, 12054−12063

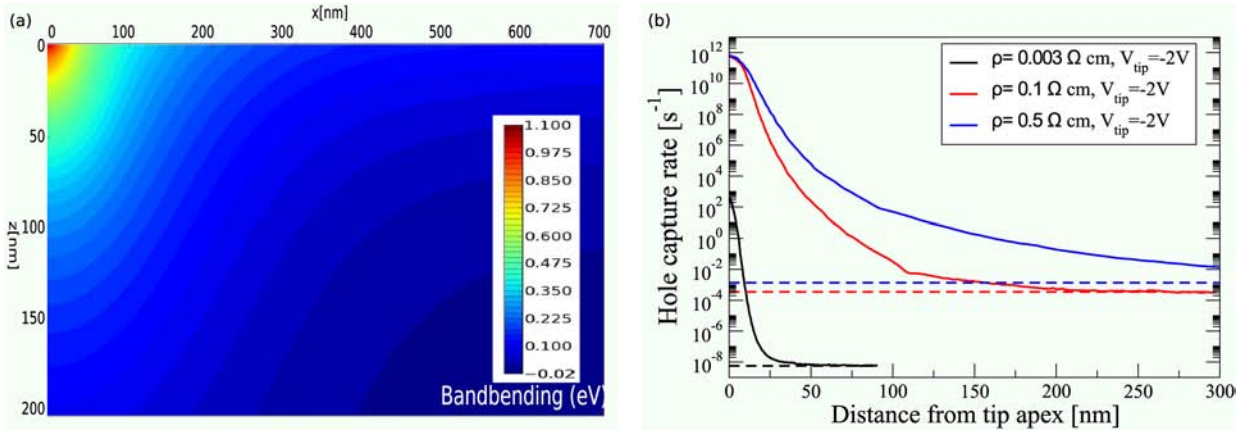

Figure 7. (a) Two-dimensional contour plots of band bending (values in eV) in a H−Si crystal in the vicinity of the biased STM tip. The surface is located at z = 1 nm with z increasing toward the sample bulk. The STM tip has a radius of 20 nm and its apex at the origin (x = z = 0). The calculation is for a surface DB density =10^{12} cm^{-2}, sample resistivity 0.5 Ωcm and tip bias −2 V. The solid blue line in (b) shows the solution for R_{rec} as a function of lateral position on the surface resulting from the band bending calculation given in (a). Solid red and black lines in (b) show the corresponding solutions returned from calculations of the band bending in samples of resistivity 0.1 and 0.003 Ω cm, respectively. The color-matching dashed lines show the corresponding recombination rates in the absence of the STM tip.

form a carbocation on the H−Si surface. To investigate this process we employ semi empirical calculations to calculate the rate of electron recombination R_{rec} with an itinerant hole of thermal velocity v_p and capture cross section σ^*_p given by

$$R_{rec} = \sigma^*_p p v_p \quad (1)$$

where p is the hole concentration at the surface and which depends (self-consistently) on the total amount of band bending at the surface due to the biased STM probe and the charging of the surface states. In order to estimate p, we solved the Poisson and Schrödinger equations in a self-consistent fashion within the semiclassical approximation. Compactly the problem can written as

$$\nabla^2 U(\mathbf{r}) = -\frac{e}{\varepsilon(\mathbf{r})}\rho_{total}(U(\mathbf{r})) \quad (2)$$

where U is the electric potential, ρ_{total} the total charge density having a functional dependence on U, and ε is the permittivity function. In Figure 7a, we show a contour plot that results from the semi classical solution for the band bending calculated for an LD hydrogen terminated silicon surface (resistivity 0.5 Ωcm) with a surface concentration of DBs (N_{DB} = 10^{12} cm^{-2}) in the vicinity of a biased STM tip (−2.0 V) of radius 20 nm separated 1 nm from the surface. The corresponding solution for R_{rec} is plotted as a solid blue line in Figure 7b and compared to R_{rec} solutions obtained with the same tip and DB density parameters for MD and HD samples, respectively.

For sample resistivity higher than 0.5 Ω cm, we encountered difficulties of converging our iterative finite element calculations, possibly due to numerical instabilities associated with a great variance in element sizes. However, the trends for the hole concentrations (and recombination rates) with increasing sample resistivity and tip voltage emerge clearly from our calculations. From Figure 7b, we see that the electron−hole recombination rates under the tip greatly increase as the sample doping level decreases. Furthermore, and consistent with the lateral range over which tip established reactivity modulation of CBMK molecule is observed on samples of varying dopant concentration (see Figure 3), R_{rec} curves exhibit minimal decay length for samples with lowest resistivity. Given that under zero bias perturbation quasi ordered nanostructures result from the CBMK reaction on an LD H−Si surface, we may infer, using Figure 7b that recombination rates at least in excess of 10^{-3} events s^{-1} are required for CBMK carbocation formation and consequent ordered assembly of the molecule on the H−Si surface. For our real LD samples, we can expect even greater and more spatially extended recombination rates. We note that such recombination rates greatly exceed the refilling rates (R_{refill}) of the C* state (by capture of an itinerant electron from an electron-depleted region in silicon) and consequently the probability of having a carbocation is very close to 1 (equal to $R_{rec}/(R_{rec} + R_{refill})$). We also calculated the subsurface band bending for cases of a positive tip (see SI). As expected in that case, the hole concentrations and the recombination rates under the tip are actually decreased compared to bulk values, while the probability of doubly occupied DBs is strongly increased.

DISCUSSION

The semiempirical results presented above suggest that recombination rates on n-type H−Si surfaces will be significantly higher under tip established conditions of positive sample bias with hole concentration and area of perturbation to be maximum on samples of high resistivity. Mechanistically, we offer that when recombination rates allow, two reaction pathways distinguishable at the instance of molecular addition, facilitate the establishment of a bound CBMK carbocation. Pathway 1 is applicable on the occasion that the CBMK molecule reacts with a neutral DB site where formation of a CBMK radical intermediate with sufficient lifetime to undergo (green arrow in Figure 6b) a thermodynamically driven inelastic electron transition between the C* electron and subsurface hole will result in the bound carbocation moiety. The alternative, pathway 2, is applicable on the occasion that the CBMK molecule encounter a positive DB site established before reaction by an earlier recombination event. The addition reaction under such conditions can proceed through dative bond formation between the DB positive site and the oxygen atom on the CBMK molecule with consequences identical to pathway 1. Mindful that the lifetime of the neutral CBMK intermediate is rather short (dechemisorption energy of 10.2 kcal/mol by our DFT calculations) and that the dative addition

dx.doi.org/10.1021/ja3017208 | J. Am. Chem. Soc. 2012, 134, 12054−12063

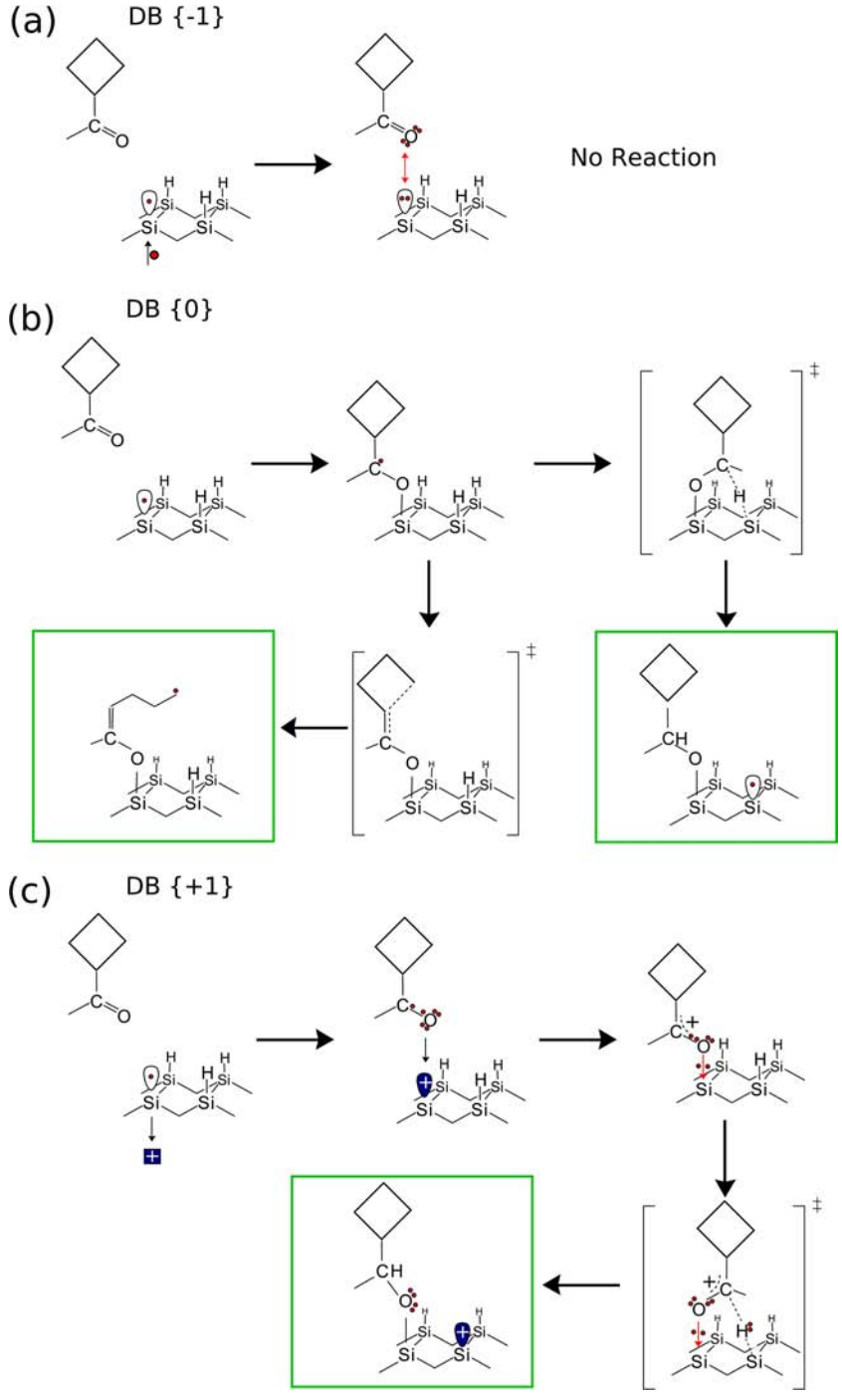

Figure 8. (a,b) and (c) are reaction schematics respectively show the outcome of the CBMK on H−Si reaction on occasion that the molecule encounter negative, neutral or positive DB centers. In (a) electrostatic repulsion between the CBMK molecule and a negatively charged DB frustrates the participation of of the CBMK molecule in radical mediated assembly and negligible product is formed. In (b), the absence of a tip field leaves most DBs neutral. In this case, the kinetics of H atom abstraction and ring-opening are comparable and both assembly modes contribute to the resulting quasi ordered products observed following reaction of the molecule on the H−Si surface (see also 2). In (c) electron hole recombination facilitates the fabrication of positive DB sites. The reaction with the CBMK molecule is through a dative bond resulting in a tethered carbocation intermediate. Ring-opening for the carbocation is inhibited but hydride atom abstraction from an adjacent site is facile resulting in the assembly of well ordered nanostructures on the surface.

to a DB positive site is barrierless we expect that pathway 2 is the more probable route to carbocation formation for the CBMK reaction on H−Si.

From the results of our DFT calculations and semiempirical model discussed above, formal mechanisms illustrating the assembly of the CBMK molecule on H−Si with DBs of assorted occupation can be proposed. In Figure 8a,b and c, appropriate reaction schematics are provided that respectively show the outcome of the CBMK on H−Si reaction on occasion that the molecules encounter negative, neutral or positive DB centers. In Figure 8a, appropriate under condition of negatively bias surface and increasingly likely on n-type H−Si surfaces of

dx.doi.org/10.1021/ja3017208 | J. Am. Chem. Soc. 2012, 134, 12054−12063

high dopant concentration, DBs will hold 2 electrons and a formal negative charge. The resulting electrostatic repulsion between the DB center and the CBMK molecule frustrates formation of the addition intermediate and prevents nanostructure formation. On occasion that the molecule encounters a neutral DB center (Figure 8b) typical under conditions of negligible tip perturbation of surface electronic states and increasingly likely on n-type H−Si samples of low dopant concentration, reaction of the molecule at the surface DB occurs through radical addition to the C═O CBMK bond and forms a neutral radical moiety that may proceed to subsequent reaction along two independent pathway viz, hydrogen abstraction leading to linear nanostructures or ring-opening followed by hydrogen abstraction leading to disordered nanostructures. The resulting quasi ordered growth observed on the surface can be understood as a consequence of the comparable kinetics associated with each of the reaction pathways navigated by the addition intermediate (see Figure 2).

In Figure 8c, appropriate under conditions of positive sample bias and increasingly probable on n-type H−Si samples of low dopant density, electrons held in neutral DB on the surface have a high probability to undergo recombination events with subsurface holes. A bonding interaction between a positive DB center and the CBMK molecule may be established with a dative bond (red arrow) where the pair of bonding electrons originate from an oxygen lone pair. The resulting carbocation intermediate is unlikely to undergo ring-opening but can abstract with relatively high probability an adjacent surface-bound hydrogen. On quenching of the carbocation, rehybridization within the tethered molecule allows the Si−O dative bond to transform to a covalent σ bond with concomitant restoration of the oxygen lone pairs. The positive DB center adjacent to the tethered molecule facilitates chain reaction chemistry and ordered nanostructure formation.

We did consider a number of alternative mechanisms for our observations, including the possibility that direct field effects were responsible for influencing the surface chemistry. Incorporating large field gradients within our DFT simulations revealed little or no change to the barrier heights associated with the critical reaction steps, leading us to conclude that field effects could not be responsible for our findings.

In conclusion, we have demonstrated DB occupancy modulation with an STM tip and showed that the CBMK/H−Si reaction acts as an excellent reporter detailing how tip established band modulation governs DB occupation on said surface. We have shown that the competition kinetics of the CBMK reaction with governance over nanostructure formation allows evaluation of how user defined DB occupancy modulation scales with sample resistivity. In addition we have demonstrated a new manipulation technique over radical mediated chain reaction chemistry on H−Si and expect that further studies tuning the potential of our STM tip will provide new paradigms to be exploited in lithographic approaches to the self-assembly reaction. Finally, we have determined that a variation on the radical mediated chain reaction chemistry on H−Si namely dative bonding with resulting carbocation formation and hydride abstraction is a viable process under certain regimes and foresee that comprehension of the new chemical process will further progress efforts in the bottom up fabrication of nanoelectronic architecture.

■ ASSOCIATED CONTENT

Supporting Information

More details of our calculations on (i) the self-consistent solution for band bending in the semiconductor due to the presence of a biased STM tip, charged DBs, and adsorbed molecules and (ii) the quantum chemical properties of relevant model systems associated with different stages of reaction of CBMK on the silicon surface. This material is available free of charge via the Internet at http://pubs.acs.org.

■ AUTHOR INFORMATION

Corresponding Author

*Gino.DiLabio@nrc.ca; rwolkow@ualberta.ca

Notes

The authors declare no competing financial interest.

■ ACKNOWLEDGMENTS

We thank Dr. Paul Piva, Dr. Jason Pitters, and Mr. Martin Cloutier for valuable discussion and assistance during this work. This work was made possible through iCORE funding.

■ REFERENCES

(1) Pitters, J. L.; Wolkow, R. A. *J. Am. Chem. Soc.* **2004**, *127*, 48−49.
(2) Pitters, J. L.; Dogel, I.; DiLabio, G. A.; Wolkow, R. A. *J. Phys. Chem. B* **2006**, *110*, 2159−2163.
(3) Hossain, M. Z.; Kato, H. S.; Kawai, M. *J. Am. Chem. Soc.* **2008**, *130*, 11518−11523.
(4) Walsh, M. A.; Walter, S. R.; Bevan, K. H.; Geiger, F. M.; Hersam, M. C. *J. Am. Chem. Soc.* **2010**, *132*, 3013−3019.
(5) Lyding, J. W.; Shen, T. C.; Hubacek, J. S.; Tucker, J. R.; Abeln, G. C. *Appl. Phys. Lett.* **1994**, *64*, 2010−2012.
(6) Shen, T. C.; Wang, C.; Abeln, G. C.; Tucker, J. R.; Lyding, J. W.; Avouris, P.; Walkup, R. E. *Science* **1995**, *268*, 1590−1592.
(7) McEllistrem, M.; Allgeier, M.; Boland, J. J. *Science* **1998**, *279*, 545−548.
(8) Foley, E. T.; Kam, A. F.; Lyding, J. W.; Avouris, P. *Phys. Rev. Lett.* **1998**, *80*, 1336−1339.
(9) Hitosugi, T.; Heike, S.; Onogi, T.; Hashizume, T.; Watanabe, S.; Li, Z. Q.; Ohno, K.; Kawazoe, Y.; Hasegawa, T.; Kitazawa, K. *Phys. Rev. Lett.* **1999**, *82*, 4034−4037.
(10) Schofield, S. R.; Curson, N. J.; Simmons, M. Y.; Rueß, F. J.; Hallam, T.; Oberbeck, L.; Clark, R. G. *Phys. Rev. Lett.* **2003**, *91*, 136104.
(11) Piva, P.; DiLabio, G. A.; Pitters, J. L.; Wolkow, R. A. To be published.
(12) Dogel, S. A.; DiLabio, G. A.; Zikovsky, J.; Pitters, J. L.; Wolkow, R. A. *J. Phys. Chem. C* **2007**, *111*, 11965−11969.
(13) Jason, L. P.; Lucian, L.; Haider, M. B.; Robert, A. W. *J. Chem. Phys.* **2011**, *134*, 064712.
(14) Pitters, J. L.; Dogel, I. A.; Wolkow, R. A. *ACS Nano* **2011**, *5*, 1984−1989.
(15) Piva, P. G.; DiLabio, G. A.; Pitters, J. L.; Zikovsky, J.; Rezeq, M.; Dogel, S.; Hofer, W. A.; Wolkow, R. A. *Nature* **2005**, *435*, 658−661.
(16) Livadaru, L.; Xue, P.; Shaterzadeh-Yazdi, Z.; DiLabio, G. A.; Mutus, J.; Pitters, J. L.; Sanders, B. C.; Wolkow, R. A. *New J. Phys.* **2010**, *12*, 083018.
(17) Lüth, H. *Solid Surfaces, Interfaces and Thin Films*; Graduate Texts in Physics; Springer: Berlin Heidelberg, 2010; pp 323−376.
(18) Bellec, A.; Riedel, D.; Dujardin, G.; Boudrioua, O.; Chaput, L.; Stauffer, L.; Sonnet, P. *Phys. Rev. B* **2009**, *80*, 245434.
(19) Livadaru, L.; Pitters, J.; Taucer, M.; Wolkow, R. *Phys. Rev. B* **2011**, *84*, 205416.
(20) Haider, M. B.; Pitters, J. L.; DiLabio, G. A.; Livadaru, L.; Mutus, J. Y.; Wolkow, R. A. *Phys. Rev. Lett.* **2009**, *102*, 046805−4.
(21) Stroscio, J.; Eigler, D. *Science* **1991**, *254*, 1319−1326.
(22) Avouris, P. *Accounts of Chemical Research* **1995**, *28*, 95−102.

(23) Lyo, I.; Avouris, P. *Science* **1991**, *253*, 173−176.
(24) Hla, S.; Meyer, G.; Rieder, K. *ChemPhysChem* **2001**, *2*, 361−366.
(25) Alemani, M.; Peters, M.; Hecht, S.; Rieder, K.; Moresco, F.; Grill, L. *J. Am. Chem. Soc.* **2006**, *128*, 14446−14447.
(26) Morgenstern, K. *Acc. Chem. Res.* **2009**, *42*, 213−223.
(27) Lorente, N.; Rurali, R.; Tang, H. *J. Phys.: Condensed Matter* **2005**, *17*, S1049.
(28) Hla, S.; Rieder, K. *Annu. Rev. Phys. Chem.* **2003**, *54*, 307−330.
(29) Riedel, D.; Mayne, A.; Dujardin, G. *Phys. Rev. B* **2005**, *72*, 233304.
(30) Lopinski, G. P.; Wayner, D. D. M.; Wolkow, R. A. *Nature (London)* **2000**, *406*, 48−51.
(31) Zikovsky, J.; Dogel, S. A.; Sinha, S.; DiLabio, G. A.; Wolkow, R. A. *Chem. Phys. Lett.* **2008**, *458*, 117−121.
(32) Beckwith, A. L. J.; Moad, G. *J. Chem. Soc., Perkin Trans. 2* **1980**, 1083−1092.
(33) Tong, X.; DiLabio, G. A.; Clarkin, O. J.; Wolkow, R. A. *Nano Lett.* **2003**, *4*, 357−360.
(34) Boland, J. J. *Adv. Phys.* **1993**, *42*, 129−171.
(35) Frisch, M. J.;et al. *Gaussian 03*, Revision D.01; Gaussian, Inc.: Wallingford, CT, 2004.
(36) Hamprecht, F. A.; Cohen, A. J.; Tozer, D. J.; Handy, N. C. *J. Chem. Phys.* **1998**, *109*, 6264−6271.
(37) DiLabio, G. A. *J. Phys. Chem. A* **1999**, *103*, 11414−11424.
(38) Mackie, I. D.; DiLabio, G. A. *J. Phys. Chem. A* **2008**, *112*, 10968−10976.
(39) Johnson, E. R.; DiLabio, G. A. *J. Phys. Chem. C* **2009**, *113*, 5681−5689.
(40) Montgomery, Jr.; F., M. J.; O., J. W., J. A.; Petersson, G. A. *J. Chem. Phys.* **2000**, *112*, 6532−6542.
(41) DiLabio, G. A.; Wolkow, R. A.; Johnson, E. R. *J. Chem. Phys.* **2005**, *122*, 044708.
(42) Tong, X.; Wolkow, R. A. *Surf. Sci.* **2006**, *600*, L199−L203.
(43) Soukiassian, L.; Mayne, A.; Carbone, M.; Dujardin, G. *Surf. Sci.* **2003**, *528*, 121−126.
(44) Newcomb, M. *Radicals in Organic Synthesis*; Wiley-VCH: Verlag GmbH, 2008; pp 316−336.
(45) Griller, D.; Ingold, K. U. *Acc. Chem. Res.* **1980**, *13*, 317−323.
(46) Nonhebel, D. C.; Suckling, C. J.; Walton, J. C. *Tetrahedron Lett.* **1982**, *23*, 4477−4480.
(47) These calculations use the same DFT methodology outlined in the Experimental and Computational Methods section, but utilized a CBMK intermediate on a cluster composed of 275 Si atoms arranged in three rows of seven dimers. See the SI.
(48) DiLabio, G. A.; Piva, P. G.; Kruse, P.; Wolkow, R. A. *J. Am. Chem. Soc.* **2004**, *126*, 16048−16050.
(49) Sinha, S.; Dickie, A. J.; Wolkow, R. A. *Chem. Phys. Lett.* **2009**, *469*, 279−283.
(50) The surface-CBMK intermediate dipole may be calculated by DFT and results indicate that it will be directed (positive to negative) into the surface with increasing field gradient set by the polarizability of the CBMK intermediate under conditions of reverse bias.